Published in final edited form as:
J Immunol. 2013 November 15; 191(10): . doi:10.4049/jimmunol.1300456.

Targeting F box protein Fbxo3 to control cytokine-driven inflammation

Rama K. Mallampalli[*,+,=,#], **Tiffany A. Coon**[*], **Jennifer R. Glasser**[*], **Claire Wang**[*], **Sarah R. Dunn**[*], **Nathaniel M. Weathington**[*], **Jing Zhao**[*], **Chunbin Zou**[*], **Yutong Zhao**[*], and **Bill B. Chen**[*,#]

[*]Departments of Medicine, Acute Lung Injury Center of Excellence, University of Pittsburgh, Pittsburgh, PA 15213 USA

[+]Department of Cell Biology and Physiology, The University of Pittsburgh, Pittsburgh, PA 15213 USA

[=]Medical Specialty Service Line, Veterans Affairs Pittsburgh Healthcare System

Abstract

Cytokine-driven inflammation underlies the pathobiology of a wide array of infectious and immune-related disorders. The tumor necrosis factor receptor-associated factor (TRAF) proteins have a vital role in innate immunity by conveying signals from cell surface receptors to elicit transcriptional activation of genes encoding pro-inflammatory cytokines. We discovered that a ubiquitin E3 ligase F box component, termed Fbxo3, potently stimulates cytokine secretion from human inflammatory cells by mediating the degradation of the TRAF inhibitory protein, Fbxl2. Analysis of the Fbxo3 carboxyl-terminal structure revealed that the bacterial-like ApaG molecular signature was indispensible for mediating Fbxl2 disposal and stimulating cytokine secretion. By targeting this ApaG motif, we developed a highly unique, selective genus of small molecule Fbxo3 inhibitors that by reducing TRAF protein levels, potently inhibited cytokine release from human blood mononuclear cells. The Fbxo3 inhibitors effectively lessened the severity of viral pneumonia, septic shock, colitis, and cytokine-driven inflammation systemically in murine models. Thus, pharmacological targeting of Fbxo3 might be a promising strategy for immune-related disorders characterized by a heightened host inflammatory response.

INTRODUCTION

Inflammation from a highly activated immune system underlies numerous human disorders characterized by the elaboration of large amounts of circulating pro-inflammatory cytokines. Sepsis and pneumonia, the leading causes of infectious deaths in the US, are pathognomonically linked to a burst in cytokine release, i.e. cytokine storm, from pro-inflammatory cells including macrophages, lymphocytes, and polymorphonuclear leukocytes (1) (2). This cytokine storm occurs after infection with virulent pathogens, but also in response to host cell injury or irritants that activate a multitude of receptors on immune effector cells. Under some conditions, the cytokine storm is exaggerated (hypercytokinemia) and results in a fatal immune reaction with constant activation of immune effector cells that produce sustained or supraphysiologic levels of tumor necrosis-α (TNFα), interleukin 1β (IL-β), and interleukin-6 (IL-6) that leads to severe tissue injury. If

Address Correspondence to: Rama K. Mallampalli [#] M.D., Bill B. Chen[#] Ph.D., The University of Pittsburgh, Pulmonary, Allergy, & Critical Care Medicine, UPMC Montefiore, NW 628, Department of Medicine, Pittsburgh, PA 15213, Tel.: 412-624-8900, Fax: 412-692-2260, chenb@upmc.edu, mallampallirk@upmc.edu.

left unchecked, this profound inflammatory cascade can have devastating consequences for the host.

Prior efforts on blocking cytokine-driven inflammation have focused on the use of systemic corticosteroids (3) or the development of targeted anti-inflammatory agents to specific cytokines (e.g. TNFα and IL-1β receptor antibodies) that have not improved mortality in sepsis (4). Other approaches focusing on inhibiting upstream surface receptors within T-cells (e.g. Toll 4 receptor) that relay external signals to cytokine responses have not succeeded in recent phase 3 clinical trials (5). Many of these approaches are limited as only one target (cytokine or receptor) was selected for inhibition, leaving unopposed activities of other pro-inflammatory stimuli (6). Alternatively, broad-spectrum agents such as corticosteroids directed at multiple targets have shown adverse effects in clinical trials that outweigh any potential benefit (4). Hence, these observations have sparked investigations of a final common pathway that regulates the cytokine host response irrespective of the microbial pathogen or insult (7).

The tumor necrosis factor receptor associated factors (TRAF) are crucial mediators of inflammatory, innate and adaptive immune responses and apoptotic programs (8). The TRAF proteins (TRAF1–6) are integral, intermediate elements, which transduce signals from a wide array of cell surface immune receptors to regulate cytokine synthesis (9). Notably, TRAF proteins mediate signal transduction emanating from the tumor necrosis factor receptor (TNFR) superfamily and the Toll like/interleukin-1 receptor (TLR/IL-1R) family (8). In addition, TRAF family proteins associate with the IL-1 receptor, CD40, RANK, I-TAC, and the p75 NGF receptor to transmit divergent signals (8). Specifically, TRAF2, TRAF5, and TRAF6 serve as adapter proteins that link cell surface receptors with nuclear factor κB activation that potently and rapidly triggers cytokine gene expression (10). TRAF-mediated cytokine release via this pathway can be exuberant, leading to severe effects of edema, multi-organ failure, and shock (11, 12). These observations provide opportunities for targeted inhibition of TRAFs that in turn could lessen the severity of pro-inflammatory host responses.

Ubiquitination is a well-recognized process required for cellular protein degradation (13). Ubiquitin conjugation involves a series of steps, the terminal reaction of which involves ubiquitin conjugation between the substrate's ε-amino lysine and the c-terminus. This latter step is catalyzed by a E3-ubiquitin ligase (14). F box proteins are subunits belonging to the Skp-Cullin1-F box (SCF) superfamily of ubiquitin E3 ligases that are used for substrate recognition (15). While over sixty F box proteins have been identified, only a few are well characterized. We recently uncovered the behavior of one F box protein, Fbxl2, which regulates phospholipid synthesis and cell cycle progression (16, 17). Recently, we observed that Fbxl2 is also a panreactive represser, targeting tumor necrosis factor receptor-associated factor (TRAF) 1–6 proteins for their polyubiquitination and degradation (18). These observations suggest that Fbxl2 might serve as a sentinel inhibitor of some innate and adaptive immune responses.

Here we provide the mechanistic basis that for the first time, led to the development of a family of F box protein small molecule antagonists that exert potent anti-inflammatory activity. We identified that a poorly characterized ubiquitin E3 ligase F box subunit, Fbxo3, robustly increases TRAF protein levels in cells by mediating ubiquitin-dependent degradation of Fbxl2, a pan-reactive TRAF inhibitor. Hence, we generated highly selective small molecule Fbxo3 antagonists based on the prokaryotic carboxyl-terminal ApaG molecular signature within the F box protein. These agents were sufficient to destabilize TRAFs protein levels in cells thereby profoundly decreasing cytokine secretion from human blood mononuclear cells. The unique broad-spectrum activity of these benzathine-based

derivatives was reflected by reduced inflammation in several complementary murine models of cytokine-driven tissue injury.

MATERIALS AND METHODS

Materials

The sources of the transformed murine lung epithelial (MLE) cell line and U937 cells lines were described previously (19–22). Purified SCF^{Fbxo3} complex was purchased from Abnova. Purified bovine calmodulin, ubiquitin, E1, E2, MG132, leupeptin, and cycloheximide were purchased from Calbiochem. Mouse monoclonal V5 antibody, the pcDNA3.1D cloning kit, *E. coli* One Shot competent cells, the pENTR Directional TOPO cloning kits, and the Gateway mammalian expression system were from Invitrogen. The F box protein cDNAs were purchased from OpenBiosystems. Nucleofector transfection kits were from Amaxa. Immobilized protein A/G beads were from Pierce. *In vitro* TnT kits were from Promega. Trypan blue and cell viability counter are from Biorad. Complete proteasome inhibitors were from Roche. Fbxl2 antibody was from Aviva Biosciences. Fbxo3 and all TRAFs antibodies were from Santa Cruz. IL1β, TNFα, IL6, human cytokine array kits were from R&D systems. All DNA sequencing was performed by the University of Pittsburgh DNA Core Facility. All small molecule compound analysis was performed by University of Pittsburgh Mass Spectrometry and NMR facility.

Cell culture

MLE cells were cultured in Dulbecco's Modified Eagle Medium-F12 (Gibco) supplemented with 2–10% fetal bovine serum (DMEM-2 or 10). U937 cells were cultured in RPMI medium supplemented with 10% fetal bovine serum. For drug treatment, compounds were solubilized either in acetic acid or ethanol before adding to the cells for up to 18 h. Cell free media was collected and analyzed for cytokines. Cell lysates were prepared by brief sonication in 150 mM NaCl, 50 mM Tris, 1.0 mM EDTA, 2 mM dithiothreitol, 0.025% sodium azide, and 1 mM phenylmethylsulfonyl fluoride (Buffer A) at 4 °C. Human peripheral blood mononuclear (PBMC) cells (0.6 ml at 1.5×10^6/ml) were treated with 2 μg/ml lipopolysaccharide (LPS) for 16 h along with BC-1215 at different concentrations. IL1β and TNFα were monitored by ELISA to calculate the IC_{50}. For LD_{50}, U937 monocytes (0.6 ml at 1.5×10^6/ml) were treated with the small molecule at different concentrations for 16 h. Cells were then stained with trypan blue to identify dead cells, and to calculate the LD_{50}. The therapeutic index (TI) = LD_{50}/IC_{50} was then determined and plotted.

Protein interaction assay

Fbxo3 protein was immunoprecipitated from Hela cell lysates using Fbxo3 antibody and captured with protein A/G beads. Fbxo3 beads were then extensively washed using 0.5% Triton X-100/PBS buffer. Fbxo3 beads were then primed with BC-1215 at different concentrations ranging from 10^{-11} to 10^{-4} M for 1 h. Purified Fbxl2 protein was then added and incubated with Fbxo3 beads overnight. Beads were then washed and Fbxo3/Fbxl2 proteins were eluted and resolved on SDS-PAGE. The relative amounts of Fbxl2 detected in pull-downs (PD) was normalized to loading and quantified and graphically.

In vitro ubiquitin conjugation assay

The ubiquitination of V5-Fbxl2 was performed in a volume of 25 μl containing 50 mM Tris pH 7.6, 5 mM $MgCl_2$, 0.6 mM DTT, 2 mM ATP, 1.5 ng/μl E1, 10 ng/μl Ubc5, 10 ng/μl Ubc7, 1 μg/μl ubiquitin (Calbiochem), 1 μM ubiquitin aldehyde, 4–16 μl of purified Cullin1, Skp1, Rbx1, and *in vitro* synthesized Fbxo3. Reaction products were processed for V5 immunoblotting.

Molecular docking studies and compound design

The docking experiments were carried out by using LigandFit from Discovery studio 3.1. A library containing 6507 approved or experimental drugs were first used to screen potential ligands for Fbxo3-ApaG. Based on the docking and best-fit analysis of suitable ligands, benzathine was selected as a backbone to develop a series of new small molecules. We modified R1, R2, and R3 groups to optimize benzathine activity (Table 1). Size and hydrophobicity of the potential compounds were carefully evaluated though the LigandFit program to determine their interaction with Fbxo3-ApaG domains. Compounds that scored high in the docking studies were custom synthesized. Our library design was based on the following rule: As shown in Table 1, wherein R3 is a divalent linking moiety; at least one of R1 or R2 is an optionally-substituted alkyl, a substituted alkoxy, optionally-substituted aryl, optionally-substituted cycloalkyl, optionally-substituted heterocyclic, or halogen.

Compound analysis

1H spectra were acquired on a Bruker 600MHz NMR. Chemical shifts are reported as parts per million (p.p.m.) downfield from tetramethylsilane. Data are reported as follows: chemical shift, multiplicity (s=singlet, d=doublet, t=triplet, m=multiplet, b=broad), coupling constant and integration. Analytical mass spectrometry (MS) was performed using the Q-Tof Ultima API Micromass mass spectrometer. The collected MS profiles were further analyzed by extracting specific ions such as 395.22 (BC-1215) in the positive ion MS mode. BC-1215 was determined to be >99% pure by LC-MS. High-resolution mass spectrometry (HRMS) was performed by the University of Pittsburgh Mass Spectrometry Laboratory. ^{1}H-NMR (400 MHz, CDCl3) of BC-1215: δ = 8.68 (d, 2H), 7.95 (d, 4H), 7.75 (m, 4H), 7.42 (d, 4H), 7.27 (t, 2H), 3.85 (s, 4H), 2.82 (s, 4H), 1.68 (s, H2O) p.p.m. HRMS (ESI) = *m/z* calculated for $C_{26}H_{26}N_4$ $[M+H]^+$ 395.2236, found 395.2220.

Quantitative RT–PCR, cloning, and mutagenesis

Total RNA was isolated and reverse transcription was performed followed by quantitative real-time PCR with SYBR Green qPCR mixture as described (23). All mutant Fbxo3 constructs were generated using PCR-based approaches using appropriate primers and subcloned into a pcDNA3.1D/V5-His vector.

Animal studies

Sepsis model—Male C57LB/6 mice (Jackson Laboratories) were acclimated at the University of Pittsburgh Animal Care Facility and maintained according to all federal and institutional animal care guidelines and under a University of Pittsburgh Institutional Animal Care and Use Committee approved protocol. Mice were deeply anesthetized with ketamine (80 to 100 mg/kg of body weight, i.p.) and xylazine (10 mg/kg, i.p.). Various amounts (500 μg, 100 μg, 20 μg, 4 μg and 0.8 μg) of BC-1215 was administered to mice though an i.p. injection. 10 min later, mice were given 100 μg of LPS (*E. coli*) through an i.p. injection. 90 min later, mice were euthanized. Plasma was collected and processed for cytokine assays.

Pneumonia model—C57BL6 mice were deeply anesthetized as above and then the larynx was well visualized under a fiber optic light source before endotracheal intubation with a 3/400 24-gauge plastic catheter. H1N1 (A/PR/8/34, 10^5 pfu/mouse) was instilled i.t. and mice monitored for up to 9 d. For BC-1215 treatment, a stock solution (5 mg/ml) was added to drinking water (containing 2% sucrose) to the final concentration of 30 μg/ml. Lung mechanics were measured at day 5 using a FlexiVent. For survival studies, mice were administered H1N1 (10^5 pfu/mouse, 8 mice/group, i.t.). Mice were carefully monitored over time; moribund, preterminal animals were immediately euthanized and recorded as deceased.

Extremity edema model—For paw edema studies, C57BL6 mice were deeply anesthetized as above. Mice were received subplantar administration of 25 μl of saline (control) or 25 μl of carrageenan (1%, w/v) in saline. Some mice were also administered 100 μg of BC-1215 (i.p.) daily. Mice were then euthanized after 48 h; the thickness and volume of paw was then measured (24).

Colitis model—Mice were fed with water containing 3.5% dextran sulfate sodium (DSS) for up to five days. Mice were treated with either vehicle or 100 μg of BC-1215 daily (via an i.p. injection). Mice were then euthanized; the colon was measured and processed for H&E and Alcian blue staining. Colonic tissues were also analysed for cytokines (25).

Ear model—20 μl of ethanol solution of BC-1215 was applied to ears at 8, 40, 200 ug/ear 30 min after TPA administration (2 μg/ear). Comparisons included equal volumes of ethanol (vehicle control). 18 h after TPA administration, mice were euthanized; the thickness of the ear was measured using a micrometer and ear punch biopsies were isolated and weighed.

Statistical analysis

Statistical comparisons were performed with the Prism program, version 4.03 (GraphPad Software, Inc., San Diego, CA) using an ANOVA 1 or an unpaired 2 t-test with $p<0.05$ indicative of significance.

RESULTS

Fbxo3 domain analysis and inhibitor screening

Fbxo3 harbors a 125 amino acid bacterial-like ApaG domain within its carboxyl-terminus, the function of which is unknown. Structural analysis from different ApaG proteins show a fold of several beta-sheets (26). Since F box proteins often utilize their carboxyl-terminal domain to target their substrates (27), we hypothesized that the Fbxo3 ApaG domain is involved in Fbxl2 recognition. Fbxl2, acting as a SCF E3 ligase component, was observed to potently inhibit lipopolysaccharide (LPS)-stimulated cytokine secretion from cells by mediating the ubiquitination and degradation of TRAFs 1–6 (18). Further, we identified that c-terminal of Fbxl2 is required for TRAFs protein targeting (Supplementary Figure S1). Using an unbiased screen of F box ubiquitinylating activity, only Fbxo3 was observed to mediate Fbxl2 ubiquitination and degradation (18). To evaluate Fbxo3 targeting of Fbxl2, we first designed a series of *Fbxo3* plasmid deletion mutants where the ApaG domain was deleted (Fig. 1A). We used *in vitro* transcription and translation (TnT) to synthesize these mutants and tested them in the *in vitro* ubiquitination assay using Fbxl2 as a substrate. Interestingly, Fbxo3-C278, which lacks the ApaG domain, lost the ability to induce polyubiquitination of Fbxl2 (Fig. 1B); Fbxo3-N70, which lacks the NH_2-terminal F box domain required to interact with the SCF complex, served as a negative control. These experiments suggest that the Fbxo3-ApaG domain is required for Fbxl2 targeting.

Next we hypothesized that inhibition of the ApaG domain disrupts Fbxo3 targeting to its substrate, Fbxl2. We first performed a structural homology analysis and identified that the Fbxo3-ApaG domain is highly conserved (Fig. 1C) (28). Using molecular docking analysis and scored-ranking operations on the predicted Fbxo3-ApaG three-dimensional structure model (28), we assessed potential ligands that might fit the ApaG domain cavities. A library containing 6507 approved or experimental drugs were first used to screen potential ligands for Fbxo3-ApaG. Based on our docking and best-fit analysis of suitable ligands, we selected benzathine as a backbone to develop a series of new small molecules (Fig. 1D). In this model, Glu^{64} within the ApaG domain (123AA) is potentially important for interacting inhibitors (Fig. 1E–F). We synthesized fourty distinct small molecules that were tested for

their half maximal inhibitory concentration (IC_{50}), half maximal lethal concentration, 50% (LC_{50}), and therapeutic index (TI= LC_{50}/IC_{50}). Importantly, one new small molecule, termed BC-1215, scored high on docking studies with Fbxo3-ApaG, which exhibited low IC_{50} and a high LC_{50} *in vitro* (Fig. 1D). (Supplementary Figure S2). Specifically, benzathine had an IC_{50} for IL-1β=25 μg/ml, LC_{50}=400 μg/ml, and TI=16; in contrast, BC-1215 had an IC_{50} IL1β=0.9 μg/ml, LD_{50}=90 μg/ml, and TI=100. In view of the favorable bioactivity and toxicity profile, this specific agent warranted further biological testing.

BC-1215 inhibits the Fbxo3-TRAF activation pathway for cytokine release

Fbxo3 protein was immunoprecipitated from Hela cell lysates using Fbxo3 antibody and captured with protein A/G beads. Fbxo3 beads were then extensively washed using 0.5% TritonX100-PBS buffer. Fbxo3 beads were then primed with BC-1215 at different concentrations ranging from 10^{-11} to 10^{-4} M before incubation with Fbxl2 for overnight. Beads were then washed and F box protein complexes were eluted and resolved on SDS-PAGE. Bound Fbxl2 protein was quantified and normalized to Fbxo3 input. Using these methods, BC-1215 exhibited maximal inhibitory binding at 10^{-7} M (Fig. 2A). Next, the ability of BC-1215 to impair Fbxo3 ubiquitination of Fbxl2 was tested using an *in vitro* ubiquitination assay. BC-1215 prevented SCF^{Fbxo3} catalyzed Fbxl2 ubiquitination with inclusion in the reaction mixture with an estimated $IC_{50}=10^{-7}$ M (Fig. 2B). To evaluate BC-1215 in cells, we first observed that the small molecule increased immunoreactive Fbxl2 levels and reduced TRAF proteins over a range of concentrations when compared to a control, benzathine (18). Other known Fbxl2 substrates including cyclin D2, cyclin D3, and cytidylyltransferase (CCT) that served as positive controls also were reduced after BC-1215 exposure (Fig. 2C). MLE cells were also co-treated with BC-1215 and TNFα. As shown in Fig. 2D, TNF treatment up-regulates TRAF2 and TRAF3 protein levels, and activates the downstream p38 and p-IKK in the NF-κB pathway. BC-1215 was able to suppress such effects in a dose-dependent manner (Fig. 2D).

BC-1215 reversibly inhibits Fbxo3 to destabilize TRAF proteins

Murine lung epithelial (MLE) cells were treated with BC-1215 at 10 μg/ml for 16 h before exposure to cycloheximide (CHX) for half-life analysis. Cells were also treated with BC-1215 at different concentrations for 16 h before assaying for TRAFs protein mRNA levels. BC-1215 decreased TRAF 1–6 protein half-life from 8–12 h to 3–4 h (Fig. 3A–B), without altering TRAF steady-state mRNA levels (Fig. 3C). To test the binding between Fbxo3 and BC-1215, *in vitro* TnT synthesized Fbxo3 proteins were first incubated with BC-1215 at 1 mg/ml. The samples were then subjected to one or three rounds of ultrafiltration, using a Microcon-YM3 filter (3 kDa cutoff, Millipore). After spinning, the protein complex was resuspended to the original volume and incubated with Fbxl2 protein. Finally, the Fbxo3/Fbxl2 protein complex was pulled down using Fbxo3 antibody and protein A/G beads before processing for immunoblotting. Using these methods, BC-1215 inhibition of Fbxo3 was reversible (Fig. 3D). These results with BC-1215 on the Fbxo3-TRAF pathway set the stage for testing of anti-inflammatory effects. In this regard, BC-1215 did not alter COX-2 activity compared to the positive control, DuP-697, a selective cyclooxygenase-2 inhibitor (Fig. 3E). BC-1215 was also incubated with purified COX-1, COX-2 and LOX-1 proteins before assaying for their enzymatic activity. As shown in Fig. 3F, at 10 μM, BC-1215 does not cause significant inhibitory effects on activities of these enzymes. Further, when MLE cells were treated with BC-1215 at different concentrations, the small molecule did not alter immunoreactive COX-2 levels (Fig. 3G). These results strongly suggest that BC-1215 mechanistically exerts anti-inflammatory signaling independent of actions by nonsteroidal anti-inflammatory drugs.

BC-1215 exhibits anti-inflammatory activity

To assess *in vitro* anti-inflammatory activity, BC-1215 (10 μg/ml) was added to LPS-treated (2 μg/ml) PBMC for 16 h and cytokine release analysis was performed. BC-1215 remarkably suppressed the majority of the Th_1 panel cytokines including G-CSF, GM-CSF, GROα, I-309, IL1-α, IL1-β, IL1rα, IL-6, IL-12, IL-23, MIP-1α, MIP-1β and TNFα (Supplementary Figure S3). Based on the unique mechanism of action of BC-1215, we next tested the effectiveness of this agent in several models of cytokine-driven inflammation in mice.

For a sepsis model, the compound was solubilized in water using acetic acid in a 1:2 molar ratio; the stock solution of BC-1215 was 5 mg/ml. BC-1215 was administered to mice at various doses through an intraperitoneal (i.p.) injection, and 10 min later, mice were given LPS (*E. coli*, 100 μg i.p.). 90 min later, mice were euthanized; blood was collected and assayed for IL1-β, IL-6 and TNFα cytokine levels. BC-1215 exhibited high potency *in vivo* (inhibitory dose [ID_{50}] IL-1β = 1 mg/kg, ID_{50} IL-6 = 2.5 mg/kg, ID_{50} TNFα = 1.2 mg/kg,) (Fig. 4A). These inhibitory concentrations are very low given that the predicted mouse oral LD_{50} doses for BC-1215 are at ~1.135 g/kg; thus, BC-1215 exerts bioactivity well below a predicted toxic dose *in vivo*. As a complementary model, we also tested BC-1215 in a mouse paw edema model to further confirm its anti-inflammatory activity. Mice received subplantar administration of saline (25 μl) or carrageenan (25 μl of 1% solution in saline) (24), followed by an i.p. injection of BC-1215 (100 μg) daily. Mice were euthanized 48 h later and the thickness and volume of the paw was measured. Paw edema was observed in carrageenan-treated animals at 48 h, however, BC-1215 was able to significantly reduce grossly and objectively paw thickness and edema compared to vehicle control (Fig. 4B–D).

BC-1215 ameliorates H1N1 influenza-induced lung injury

To further test BC-1215 in pneumonia, mice were challenged with H1N1 (10^5pfu/mouse, i.t.) and observed for 9 d. For BC-1215 treatment, a stock solution (5 mg/ml) was added to drinking water (containing 2% sucrose) to the final concentration of 30 μg/ml. Lung mechanics were measured at day 5. Specifically, BC-1215 decreased lung resistance, reduced elastance (a marker of lung stiffness), and increased compliance in mice infected with H1N1 (Fig. 5A–C). Further, BC-1215 significantly increased survival of mice infected with H1N1 compared to mice receiving diluent (Fig. 5D). BC-1215 also remarkably decreased lavage cell counts, protein concentration (Fig. 5E, F), and lessened severity of pulmonary edema and hemorrhage (Fig. 5G) and alveolar inflammation (Fig. 5H). These results suggest that the Fbxo3 antagonist suppresses inflammation and preserves lung biophysical activity after pulmonary microbial infection.

BC-1215 ameliorates DSS-induced colitis

We also tested BC-1215 in a mouse colitis model to confirm its anti-inflammatory activity. Briefly, C57BL6 mice were fed with water containing 3.5% dextran sulfate sodium (DSS) *ad lib* for five days. Mice were also treated with either vehicle or BC-1215 (100 μg, i.p.) daily. Mice were euthanized and colonic length was measured. As expected, DSS produced a significant decrease in colonic length in mice, consistent with gut inflammation (Fig. 6A). However, mice treated with BC-1215 showed no significant decrease in colon length compared to control. We further analyzed colonic tissue cytokine levels. As shown in Fig. 6B–C, mice treated with BC-1215 showed a large reduction in IL1β and TNFα levels in colonic tissue compared to vehicle treated mice. Colon tissues were further assayed for TRAF protein levels. As shown in Fig. 6D, DSS increases TRAFs 1 – 4 protein levels, however, BC-1215 was able to suppress such effects with a significant reduction of immunoreactive TRAF2 and TRAF4 content. Further, H&E and Alcian staining of colon tissue indicated that BC-1215 produced significant restoration of colonic crypts with

reappearance of goblet cells compared to the vehicle control (Fig. 6E). Thus, the Fbxo3 inhibitor suppresses inflammation in a chemical induced colitis model in mice.

BC-1215 reduces TPA induced ear edema

We also tested effects of topical application of BC-1215 as an anti-inflammatory agent in a model of 12-*O*-tetradecanoylphorbol-13-acetate (TPA) induced ear edema (29). Briefly, 20 μl of an ethanol solution of BC-1215 was applied to ears of mice at 8, 40, and 200 ug/ear for 30 min after TPA administration (2 μg/ear). Comparisons included equal volumes of ethanol (vehicle control). 18 h after TPA administration, mice were euthanized; the thickness of the ear was measured using a micrometer. Ear punch biopsies were also taken immediately, weighed, and graphed. As shown in Fig. 7A, ear edema and erythema was observed in the TPA-treated animals at 18 h after its treatment. However, BC-1215 was able to significantly resolve these findings. BC-1215 significantly reduced ear thickness and ear weight in a dose dependent manner compared to the vehicle control (Fig. 7B,C). Hence, BC-1215 exerts anti-inflammatory activity topically.

DISCUSSION

Here we developed the first generation of F box protein small molecule inhibitors that exert robust anti-inflammatory activity by impairing cytokine release in a variety of preclinical models. We have engineered the therapeutics to target a pivotal substrate, F box protein Fbxo3, which activates pro-inflammatory signaling by mediating proteasomal elimination of Fbxl2, a TRAF protein inhibitor (18). Hence, we provide the mechanistic platform that led to the design, synthesis, and biological evaluation of these agents in an array of small animal models that vary in their site of injury, yet are fundamentally linked by the role of pro-inflammatory cytokines in mediating disease pathogenesis. Our efforts began with the identification of the Fbxo3 ApaG as a unique molecular targeting signature, which led to the discovery of the compound BC-1215 as a prototypical Fbxo3 inhibitor for the generation of several additional congeners. Some of these nonpeptidic therapeutics displayed limited toxicity *in vitro*. By targeting TRAF-mediated cytokine release, these agents might have more limited adverse effects compared to corticosteroids that suppress inflammation within multiple biological pathways (30–32), but provide broader activities relative to existing anti-inflammatories targeted to a single cytokine (33–38). A therapeutic role for translation of Fbxo3 inhibitors to the clinical arena awaits additional preclinical pharmacokinetic and *in vivo* toxicity analysis.

The structural basis for our drug design emerged from benzathine, a diamine used as a stabilizer in many medications. For over fifty years, benzathine was used to stabilize penicillin and many other antibiotics to prolong their shelf life (39–41). However, there are no reports describing the use of benzathine or related derivatives as protein inhibitors or anti-inflammatory agents. We report that by adding a pyridine group to the benzathine backbone generating BC-1215, the new molecule was sufficient to profoundly inhibit inflammation in several murine models. Although structure-activity analysis led to several modified Fbxo3 antagonists that displayed potent anti-inflammatory activities, the ability of BC-1215 to decrease TRAF proteins in cells and inhibit cytokine secretion exceeded many compounds and yet displayed lower *in vitro* toxicity.

A mechanistic centerpiece for actions of Fbxo3 inhibitors is their ability to interact with the ApaG domain. This domain is present in *Xanthomonas, Vibrio*, and *Salmonella* species where it is postulated to interact with pyrophosphate, nucleotide phosphates, or heavy metals (42). It is not clear regarding the prevalence of the ApaG domain within host cellular proteins, but to date it has been only identified within some F box proteins and within PDIP38, a protein that interacts with proliferating cell nuclear antigen (43, 44). It is tempting

to speculate that given ApaG existence primarily with bacterial species, Fbxo3 targeting with small molecule inhibitors might be associated with limited off-target effects and perhaps additional bacteriocidal or bacteriostatic activity. Consistent with this premise, BC-1215 was observed to produce modest inhibition of bacterial growth using Kirby Bauer testing (*data not shown*). The validation of Fbxo3 congeners with dual activity as antimicrobial-inflammatories is novel that requires further study.

Our pre-clinical studies demonstrate biologic efficacy in models where both infectious and irritant factors trigger cytokine release. For example, H1N1 infection is largely driven by an exuberant host response from the elaboration of cytokines and chemokines that contribute to influenza-induced morbidity and mortality in people (45). This pulmonary infection model was complemented with a murine sepsis model to provide assessment of F box inhibitors on systemic inflammation by endotoxin (46). Because sepsis is associated with multi-organ failure linked to immune driven tissue injury at distal sites, we also tested BC-1215 in models of colitis, paw, and ear edema. The irritants used in these studies also trigger release of pro-inflammatory cytokines (47–49). Importantly, in each of these models of inflammation, BC-1215 was observed to lessen severity of tissue injury using varying modes of application (parenteral, oral, topical), and all animals treated with the agent were not observed to exhibit overt signs of distress. The carrageenan model, in particular, is a classic model of acute paw edema formation that has been widely used in testing of nonsteroidal anti-inflammatory drugs that act via selective cyclooxygenase inhibition. The observation that BC-1215 was efficacious in this model, independent of COX inhibitory activity, coupled with findings of elevated Fbxo3 expression in synovial tissues from subjects with rheumatoid arthritis predicts a potentially attractive role for F box protein inhibitors in chronic musculoskeletal inflammatory illness (50). However, further research and development clearly is needed to carefully ascertain the safety profile, distribution, elimination, and metabolism of these new chemical entities in larger models of inflammation. Successful results from these pharmacokinetic studies will set the stage for transition to clinical testing in subjects with acute and chronic immune-related illness.

Supplementary Material

Refer to Web version on PubMed Central for supplementary material.

Acknowledgments

We thank the Dr. Bhaskar Godugu of the MS and NMR facility at the University of Pittsburgh who assisted with chemical analysis. We thank Yingze Zhang for critical review of this manuscript.

This material is based upon work supported, in part, by the US Department of Veterans Affairs, Veterans Health Administration, Office of Research and Development, Biomedical Laboratory Research and Development. This work was supported by a Merit Review Award from the US Department of Veterans Affairs and National Institutes of Health R01 grants HL096376, HL097376 and HL098174 (to R.K.M.), HL116472 (to B.B.C.), HL01916 (to Y.Z.), and American Heart Association awards 12SDG9050005 (J.Z.) and 12SDG12040330 (C.Z.).

REFERENCES

1. Sheu CC, Gong MN, Zhai R, Bajwa EK, Chen F, Thompson BT, Christiani DC. The influence of infection sites on development and mortality of ARDS. Intensive Care Med. 2010; 36:963–970. [PubMed: 20229040]
2. Dinarello CA. Historical insights into cytokines. Eur J Immunol. 2007; 37(Suppl 1):S34–S45. [PubMed: 17972343]
3. Annane D, Cavaillon JM. Corticosteroids in sepsis: from bench to bedside? Shock. 2003; 20:197–207. [PubMed: 12923489]

4. Sweeney DA, Danner RL, Eichacker PQ, Natanson C. Once is not enough: clinical trials in sepsis. Intensive Care Med. 2008; 34:1955–1960. [PubMed: 18839140]
5. Angus DC. The search for effective therapy for sepsis: back to the drawing board? Jama. 2011; 306:2614–2615. [PubMed: 22187284]
6. Riedemann NC, Guo RF, Ward PA. Novel strategies for the treatment of sepsis. Nat Med. 2003; 9:517–524. [PubMed: 12724763]
7. Paterson RL, Galley HF, Webster NR. The effect of N-acetylcysteine on nuclear factor-kappa B activation, interleukin-6, interleukin-8, and intercellular adhesion molecule-1 expression in patients with sepsis. Crit Care Med. 2003; 31:2574–2578. [PubMed: 14605526]
8. Inoue J, Ishida T, Tsukamoto N, Kobayashi N, Naito A, Azuma S, Yamamoto T. Tumor necrosis factor receptor-associated factor (TRAF) family: adapter proteins that mediate cytokine signaling. Exp Cell Res. 2000; 254:14–24. [PubMed: 10623461]
9. Xu LG, Li LY, Shu HB. TRAF7 potentiates MEKK3-induced AP1 and CHOP activation and induces apoptosis. J Biol Chem. 2004; 279:17278–17282. [PubMed: 15001576]
10. Rickert RC, Jellusova J, Miletic AV. Signaling by the tumor necrosis factor receptor superfamily in B-cell biology and disease. Immunol Rev. 2011; 244:115–133. [PubMed: 22017435]
11. London NR, Zhu W, Bozza FA, Smith MC, Greif DM, Sorensen LK, Chen L, Kaminoh Y, Chan AC, Passi SF, Day CW, Barnard DL, Zimmerman GA, Krasnow MA, Li DY. Targeting Robo4-dependent Slit signaling to survive the cytokine storm in sepsis and influenza. Sci Transl Med. 2010; 2 23ra19.
12. Harrison C. Sepsis: calming the cytokine storm. Nat Rev Drug Discov. 2010; 9:360–361. [PubMed: 20431565]
13. Tanaka Y, Tanaka N, Saeki Y, Tanaka K, Murakami M, Hirano T, Ishii N, Sugamura K. c-Cbl-dependent monoubiquitination and lysosomal degradation of gp130. Mol Cell Biol. 2008; 28:4805–4818. [PubMed: 18519587]
14. Hochstrasser M. Biochemistry. All in the ubiquitin family. Science. 2000; 289:563–564. [PubMed: 10939967]
15. Jin J, Cardozo T, Lovering RC, Elledge SJ, Pagano M, Harper JW. Systematic analysis and nomenclature of mammalian F-box proteins. Genes Dev. 2004; 18:2573–2580. [PubMed: 15520277]
16. Chen BB, Coon TA, Glasser JR, Mallampalli RK. Calmodulin antagonizes a calcium-activated SCF ubiquitin E3 ligase subunit, FBXL2, to regulate surfactant homeostasis. Mol Cell Biol. 2011; 31:1905–1920. [PubMed: 21343341]
17. Chen BB, Glasser JR, Coon TA, C Z, HL M, Fenton M, JF M, M B, Mallampalli RK. F box protein FBXL2 targets cyclin D2 for ubiquitination and degradation to inhibit leukemic cell proliferation. Blood. 2012; 119:3132–3141. [PubMed: 22323446]
18. Chen BB, Coon TA, Glasser JR, McVerry BJ, Zhao J, Zhao Y, Zou C, Ellis B, Sciurba FC, Zhang Y, Mallampalli RK. A combinatorial F box protein directed pathway controls TRAF stability to regulate inflammation. Nat. Immunol. 2013; 14(5):470–479. [PubMed: 23542741]
19. Ray NB, Durairaj L, Chen BB, McVerry BJ, Ryan AJ, Donahoe M, Waltenbaugh AK, O'Donnell CP, Henderson FC, Etscheidt CA, McCoy DM, Agassandian M, Hayes-Rowan EC, Coon TA, Butler PL, Gakhar L, Mathur SN, Sieren JC, Tyurina YY, Kagan VE, McLennan G, Mallampalli RK. Dynamic regulation of cardiolipin by the lipid pump Atp8b1 determines the severity of lung injury in experimental pneumonia. Nat Med. 2010; 16:1120–1127. [PubMed: 20852622]
20. Chen BB, Mallampalli RK. Calmodulin binds and stabilizes the regulatory enzyme, CTP: phosphocholine cytidylyltransferase. J Biol Chem. 2007; 282:33494–33506. [PubMed: 17804406]
21. Chen BB, Glasser JR, Coon TA, Zou C, Miller HL, Fenton M, McDyer JF, Boyiadzis M, Mallampalli RK. F-box protein FBXL2 targets cyclin D2 for ubiquitination and degradation to inhibit leukemic cell proliferation. Blood. 2012; 119:3132–3141. [PubMed: 22323446]
22. Chen BB, Glasser JR, Coon TA, Mallampalli RK. F-box protein FBXL2 exerts human lung tumor suppressor-like activity by ubiquitin-mediated degradation of cyclin D3 resulting in cell cycle arrest. Oncogene. 2012; 31:2566–2579. [PubMed: 22020328]

23. Butler PL, Mallampalli RK. Cross-talk between remodeling and de novo pathways maintains phospholipid balance through ubiquitination. J Biol Chem. 2010; 285:6246–6258. [PubMed: 20018880]
24. Posadas I, Bucci M, Roviezzo F, Rossi A, Parente L, Sautebin L, Cirino G. Carrageenan-induced mouse paw oedema is biphasic, age-weight dependent and displays differential nitric oxide cyclooxygenase-2 expression. Br J Pharmacol. 2004; 142:331–338. [PubMed: 15155540]
25. Yoshihara K, Yajima T, Kubo C, Yoshikai Y. Role of interleukin 15 in colitis induced by dextran sulphate sodium in mice. Gut. 2006; 55:334–341. [PubMed: 16162679]
26. Katsuyama AM, Cicero DO, Spisni A, Paci M, Farah CS, Pertinhez TA. 1H, 15N and 13C resonance assignments of the ApaG protein of the phytopathogen Xanthomonas axonopodis pv. citri. J Biomol NMR. 2004; 29:423–424. [PubMed: 15213450]
27. Winston JT, Koepp DM, Zhu C, Elledge SJ, Harper JW. A family of mammalian F-box proteins. Curr Biol. 1999; 9:1180–1182. [PubMed: 10531037]
28. Wu S, Zhang Y. LOMETS: a local meta-threading-server for protein structure prediction. Nucleic Acids Res. 2007; 35:3375–3382. [PubMed: 17478507]
29. Bralley EE, Greenspan P, Hargrove JL, Wicker L, Hartle DK. Topical anti-inflammatory activity of Polygonum cuspidatum extract in the TPA model of mouse ear inflammation. J Inflamm (Lond). 2008; 5:1. [PubMed: 18261214]
30. Claes C, Kulp W, Greiner W, von der Schulenburg JM, Werfel T. Therapy of moderate and severe psoriasis. GMS Health Technol Assess. 2006; 2:Doc07. [PubMed: 21289958]
31. de Quervain DJ. Glucocorticoid-induced inhibition of memory retrieval: implications for posttraumatic stress disorder. Ann N Y Acad Sci. 2006; 1071:216–220. [PubMed: 16891572]
32. Foster JM, van Sonderen E, Lee AJ, Sanderman R, Dijkstra A, Postma DS, van der Molen T. A self-rating scale for patient-perceived side effects of inhaled corticosteroids. Respir Res. 2006; 7:131. [PubMed: 17062139]
33. Hansen G, Hercus TR, McClure BJ, Stomski FC, Dottore M, Powell J, Ramshaw H, Woodcock JM, Xu Y, Guthridge M, McKinstry WJ, Lopez AF, Parker MW. The structure of the GM-CSF receptor complex reveals a distinct mode of cytokine receptor activation. Cell. 2008; 134:496–507. [PubMed: 18692472]
34. Zaghi D, Krueger GG, Callis Duffin K. Ustekinumab: a review in the treatment of plaque psoriasis and psoriatic arthritis. J Drugs Dermatol. 2012; 11:160–167. [PubMed: 22270196]
35. Herrlinger K, Stange EF. Inflammatory bowel diseases--new therapeutic options. Med Klin (Munich). 2008; 103:90–101. quiz 102–103. [PubMed: 18270665]
36. Mahadevan U. TNF-alpha antagonists: benefits beyond remission. Rev Gastroenterol Disord. 2007; 7(Suppl 1):S13–S19. [PubMed: 17392633]
37. Murdaca G, Colombo BM, Puppo F. Adalimumab for the treatment of immune-mediated diseases: an update on old and recent indications. Drugs Today (Barc). 2011; 47:277–288. [PubMed: 21573251]
38. Launois R, Avouac B, Berenbaum F, Blin O, Bru I, Fautrel B, Joubert JM, Sibilia J, Combe B. Comparison of certolizumab pegol with other anticytokine agents for treatment of rheumatoid arthritis: a multiple-treatment Bayesian metaanalysis. J Rheumatol. 2011; 38:835–845. [PubMed: 21239748]
39. Laurance B. Penicillin by mouth in infancy; a comparison between benzathine and sodium penicillins. Br Med J. 1954; 2:1392–1394. [PubMed: 13209127]
40. Anderson HC. Prolonged reaction to intramuscular benzathine penicillin. Lancet. 1954; 267:1157–1158. [PubMed: 13213150]
41. REPORT on benzathine penicillin G. J Am Dent Assoc. 1954; 49:714–715. [PubMed: 13211170]
42. Chin KH, Chou CC, Lee CC, Shr HL, Lyu PC, Wang AH, Chou SH. Preparation, crystallization and preliminary X-ray analysis of XC2382, an ApaG protein of unknown structure from Xanthomonas campestris. Acta Crystallogr Sect F Struct Biol Cryst Commun. 2005; 61:700–702.
43. Ilyin GP, Rialland M, Pigeon C, Guguen-Guillouzo C. cDNA cloning and expression analysis of new members of the mammalian F-box protein family. Genomics. 2000; 67:40–47. [PubMed: 10945468]

44. Liu L, Rodriguez-Belmonte EM, Mazloum N, Xie B, Lee MY. Identification of a novel protein, PDIP38, that interacts with the p50 subunit of DNA polymerase delta and proliferating cell nuclear antigen. J Biol Chem. 2003; 278:10041–10047. [PubMed: 12522211]
45. Wang J, Nikrad MP, Travanty EA, Zhou B, Phang T, Gao B, Alford T, Ito Y, Nahreini P, Hartshorn K, Wentworth D, Dinarello CA, Mason RJ. Innate immune response of human alveolar macrophages during influenza A infection. PLoS One. 2012; 7:e29879. [PubMed: 22396727]
46. Rath HC, Schultz M, Freitag R, Dieleman LA, Li F, Linde HJ, Scholmerich J, Sartor RB. Different subsets of enteric bacteria induce and perpetuate experimental colitis in rats and mice. Infect Immun. 2001; 69:2277–2285. [PubMed: 11254584]
47. Rocha AC, Fernandes ES, Quintao NL, Campos MM, Calixto JB. Relevance of tumour necrosis factor-alpha for the inflammatory and nociceptive responses evoked by carrageenan in the mouse paw. Br J Pharmacol. 2006; 148:688–695. [PubMed: 16702985]
48. Krieglstein CF, Cerwinka WH, Sprague AG, Laroux FS, Grisham MB, Koteliansky VE, Senninger N, Granger DN, de Fougerolles AR. Collagen-binding integrin alpha1beta1 regulates intestinal inflammation in experimental colitis. J Clin Invest. 2002; 110:1773–1782. [PubMed: 12488427]
49. Yoon T, Lee do Y, Lee AY, Choi G, Choo BK, Kim HK. Anti-inflammatory effects of Glehnia littoralis extract in acute and chronic cutaneous inflammation. Immunopharmacol Immunotoxicol. 2010; 32:663–670. [PubMed: 20230179]
50. Masuda K, Masuda R, Neidhart M, Simmen BR, Michel BA, Muller-Ladner U, Gay RE, Gay S. Molecular profile of synovial fibroblasts in rheumatoid arthritis depends on the stage of proliferation. Arthritis Res. 2002; 4:R8. [PubMed: 12223111]

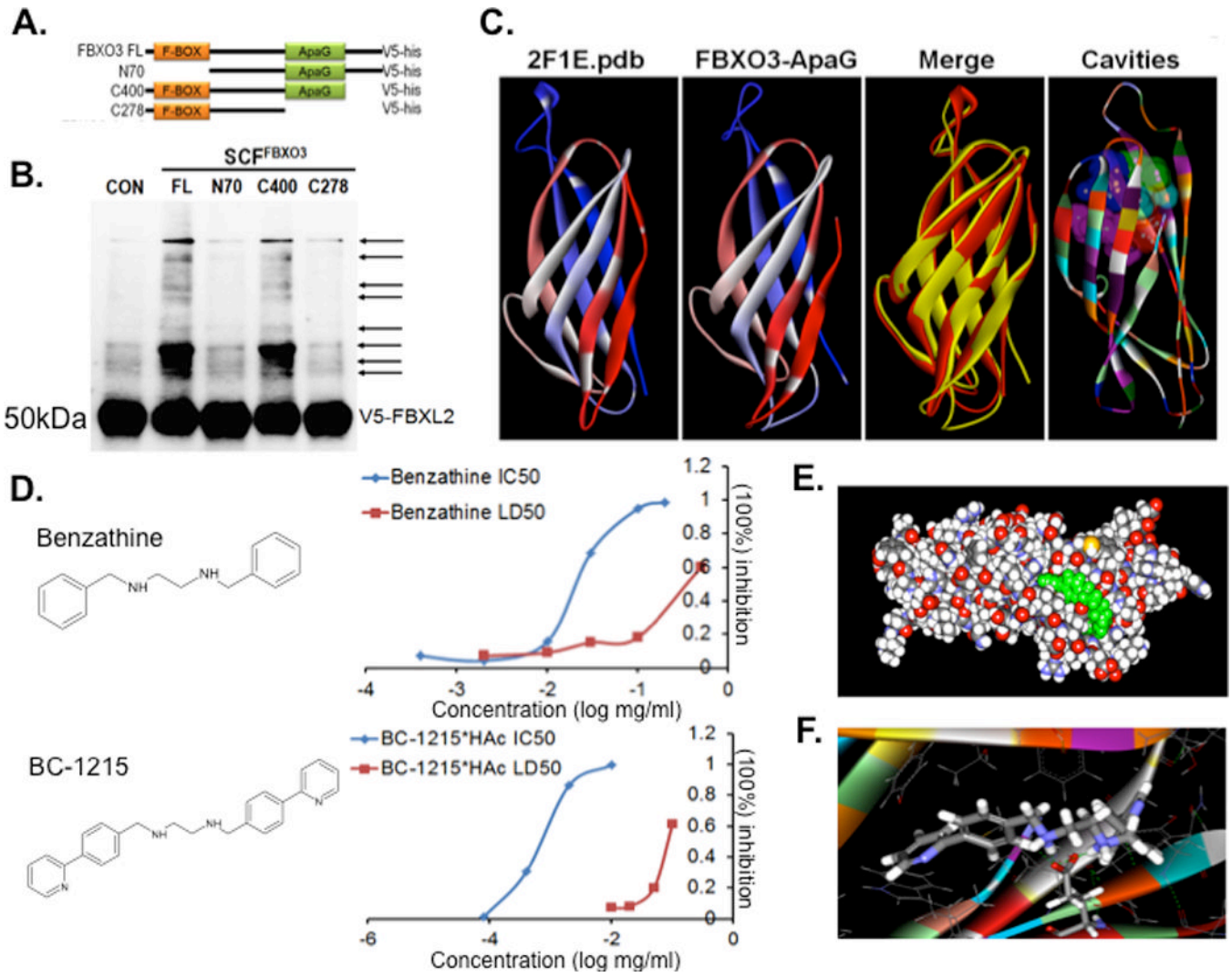

Figure 1. The ApaG Fbxo3 domain serves as a target for small molecules

A. Several deletion mutants of Fbxo3 were designed and cloned into a pcDNA3.1D/V5-HIS vector. **B.** *In vitro* ubiquitination assays. Purified SCF^{Fbxo3} full-length (FL) or truncated Fbxo3 proteins were incubated with V5-Fbxl2 substrate and the full complement of ubiquitination reaction components showing polyubiquitinated Fbxl2 (second lane from left). **C.** Structural analysis of the Fbxo3-ApaG domain showing highly conserved bacterial (left) and mammalian Fbxo3 (second from left) structures. **D.** Structure of the base compound, benzathine, and the Fbxo3 antagonist, BC-1215. Right graphs. Human peripheral blood mononuclear (PBMC) cells were treated with LPS (2 μg/ml) for 16 h along with either benzathine or BC-1215 at different concentrations and IL1β and TNFα monitored to calculate the IC_{50}. For LD_{50}, U937 monocytes were treated with the small molecules at different concentrations for 16 h. Cells were then stained with trypan blue to identify dead cells, and to calculate the LD_{50}. **E–F.** Docking studies of the base compound, benzathine, interacting with the Fbxo3-ApaG domain. Data from panel B represent n=2 separate experiments.

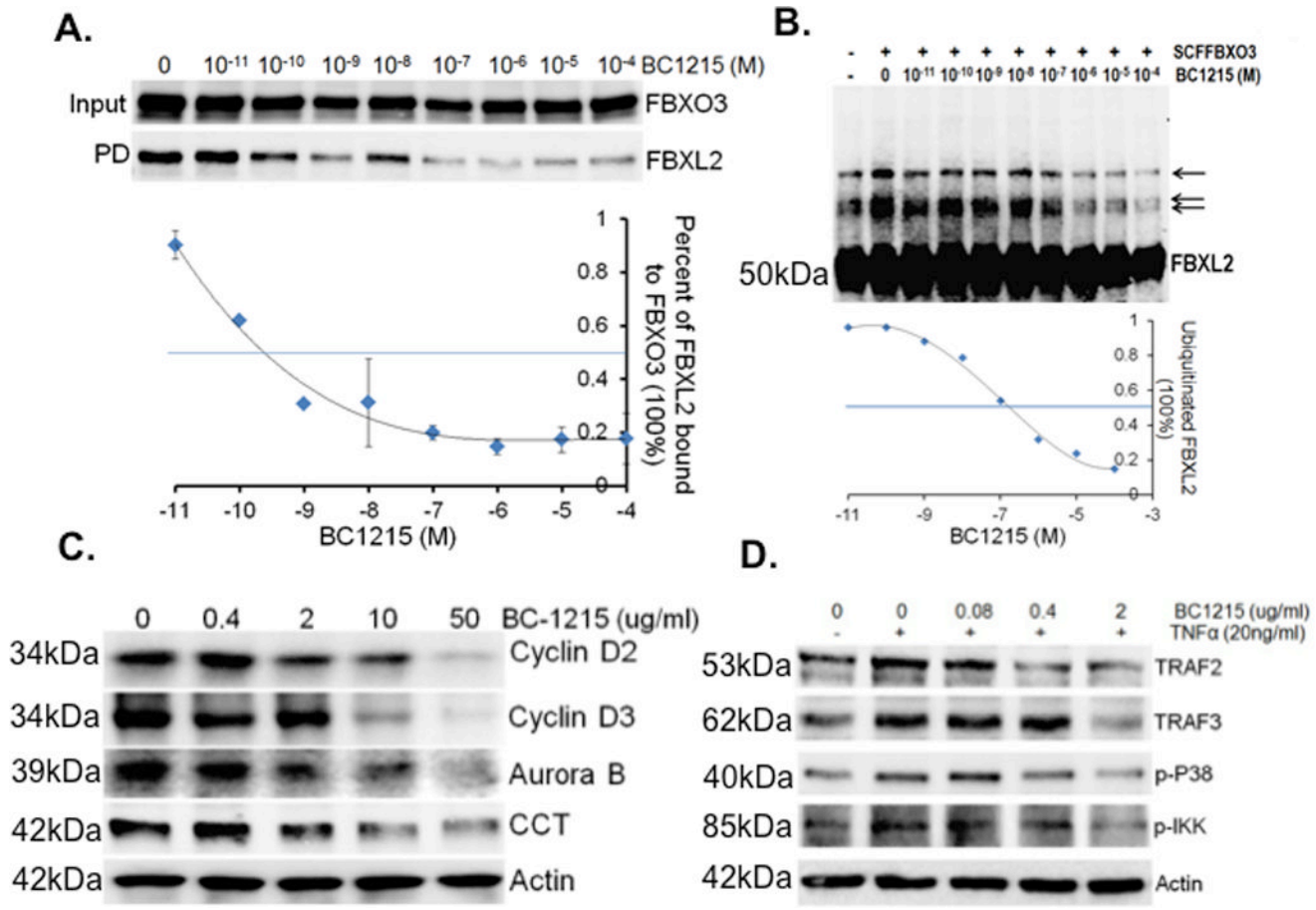

Figure 2. A small molecule inhibitor, BC-1215, inhibits Fbxo3 function

A. Fbxo3 protein was immunoprecipitated using Fbxo3 antibody and captured with protein A/G beads from Hela cell lysates. Fbxo3 beads were then extensively washed prior to exposure to BC-1215 at different concentrations (10^{-11} to 10^{-4} M). Purified FBXL2 protein was then incubated with Fbxo3 beads overnight, beads were washed, and F box complexes were eluted and resolved on SDS-PAGE. The relative amounts of Fbxl2 detected in pull-downs (PD) was normalized to loading and quantified as shown graphically below. **B.** *In vitro* ubiquitination assays. Purified SCF^{Fbxo3} complex components were incubated with V5-Fbxl2 and the full complement of ubiquitination reaction components with increased concentrations of BC-1215 or vehicle showing decreased levels of polyubiquitinated Fbxl2 (arrows). The lower graph quantifies levels of ubiquitinated Fbxl2 as a function of BC-1215 concentration. **C.** Murine lung epithelial (MLE) cells were treated with BC-1215 at different concentrations for 16 h. Cells were collected and assayed for cyclin D2, cyclin D3, Aurora B, CCT, and β actin immunoblotting. **D.** MLE cells were co-treated with BC-1215 (10 μg/ml) and TNFα (10 ng/ml) for 6 h. Cells were then collected and assayed for immunoblotting. Data from each panel represents at least n=2 separate experiments.

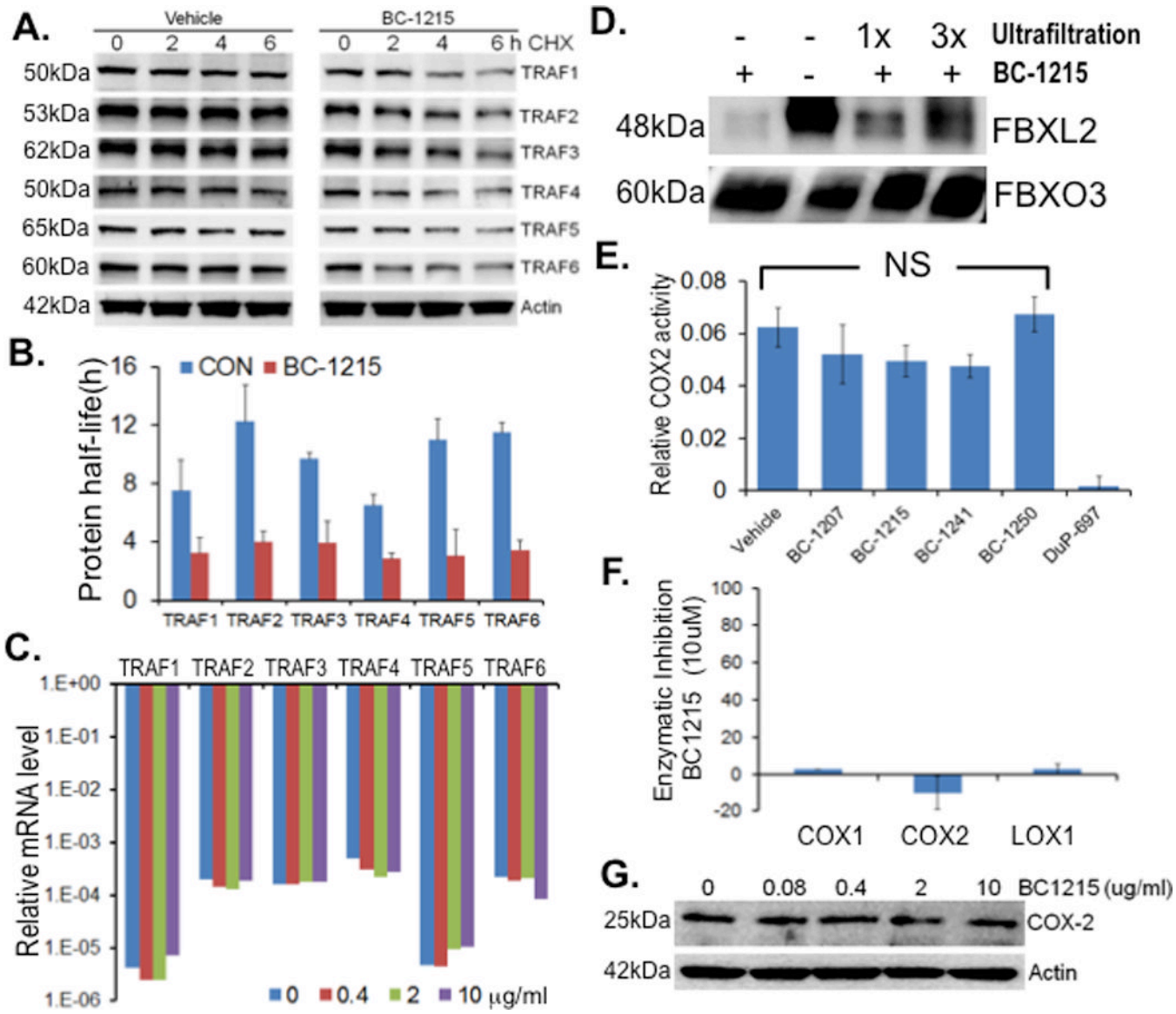

Figure 3. BC-1215 reversibly inhibits Fbxo3 resulting destabilized TRAF proteins

A. MLE cells were treated with BC-1215 at 10 μg/ml for 16 h before exposure to cycloheximide (CHX) for half-life analysis. TRAF protein levels were quantified using Image J software and half-lives were calculated and graphed in **B**. **C.** MLE cells were treated with BC-1215 at different concentrations for 16 h before assaying for TRAF mRNA levels. **D.** *In vitro* TnT synthesized Fbxo3 protein was first incubated with BC-1215 at 1 mg/ml. The sample was then subjected to one or three rounds of ultrafiltration, using a Microcon-YM3 filter (3 kDa cutoff, Millipore). After spinning, the protein complex was resuspended to the original volume and incubated with Fbxl2 protein. Finally, Fbxo3/FBbxl2 protein complex was pulled-down using Fbxo3 antibody and protein A/G beads before processing for immunoblotting. **E.** MLE cells were treated with either vehicle or benzathine derivatives (10 μg/ml) for 16 h before assaying for COX-2 activity (Cayman). **F.** BC-1215 (10 μM) was incubated with purified COX-1, COX-2 and LOX-1 proteins before assaying for their enzymatic activity. **G.** MLE cells were treated with BC-1215 at different

concentration for 16 h, cells were then collected and assayed for COX-2 levels by immunoblotting.

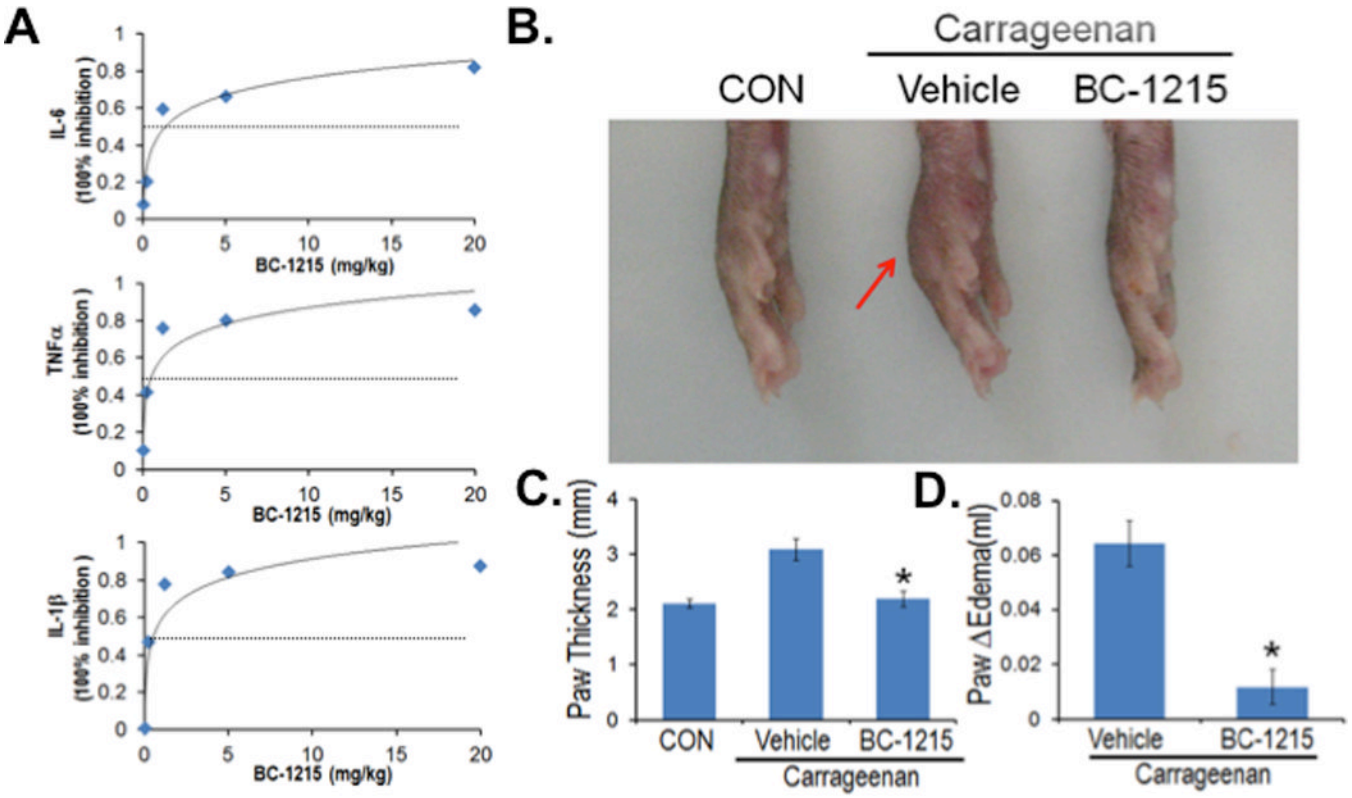

Figure 4. BC-1215 exhibits anti-inflammatory activity

A. C57BL6 mice were administered i.p. nothing (CON), vehicle, 500 μg, 100 μg, 20 μg, 4 μg and 0.8 μg of BC-1215. 10 min later, mice were given LPS (*E. coli*, 100 μg) through an i.p. injection and 90 min later mice were euthanized and blood collected for IL1-β, IL-6 and TNFα measurements. Shown in panel A is % inhibition of cytokine levels as a function of drug dose. The data represent n=3 mice/group at each dose. **B–D.** Mice received subplantar administration of saline or carrageenan (1% in saline), followed immediately by an i.p. injection of 100 μg of BC-1215 daily for two days. Mice were then euthanized, imaging performed (**B**), and the thickness and volume of the paw was measured (**C–D**). The data represent n=4–6 mice/group, and in **C–D** *P<0.05 versus vehicle.

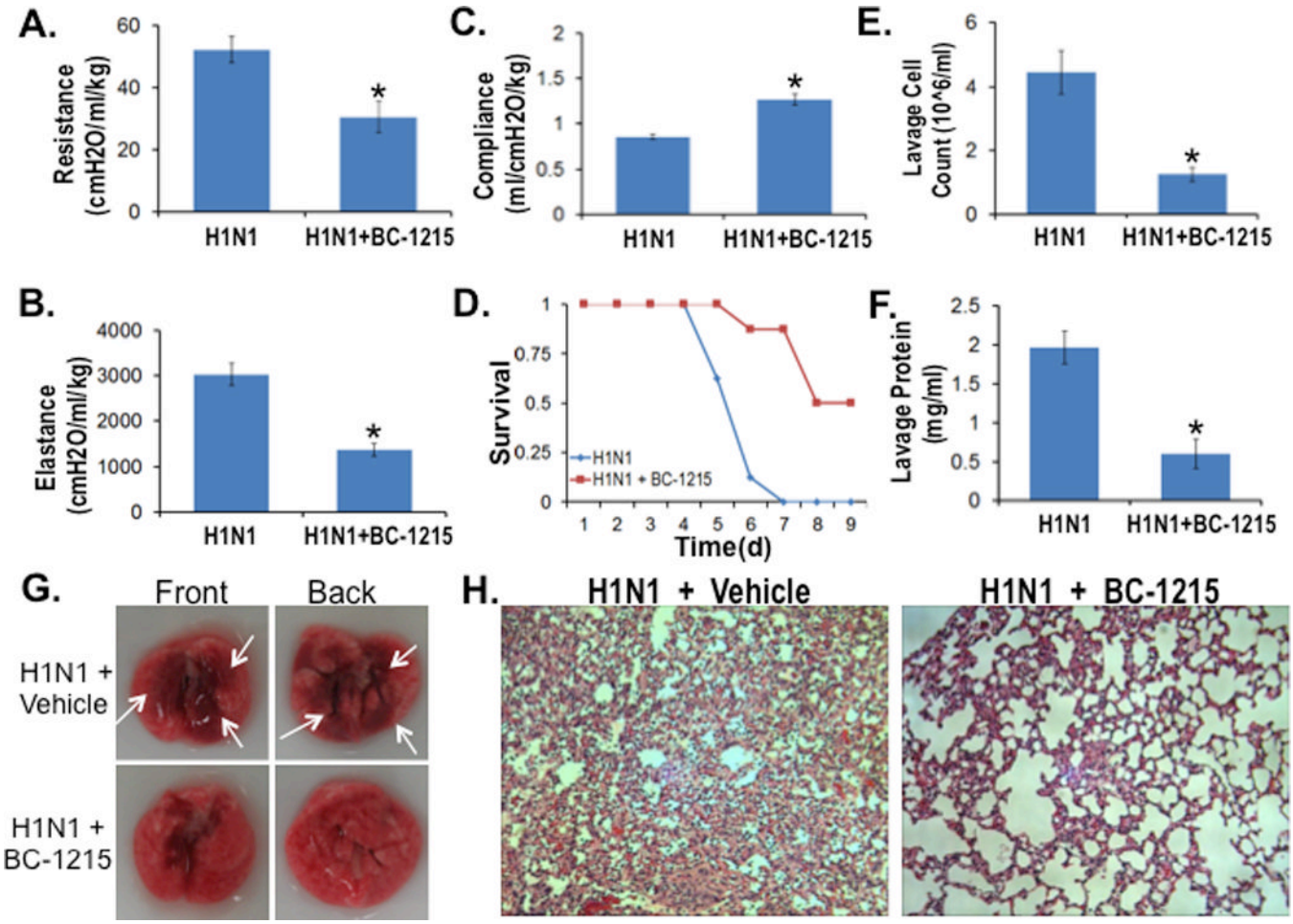

Figure 5. BC-1215 lessens severity of H1N1 influenza pneumonia

A–D. C57BL6 mice were challenged with H1N1 (10^5 pfu/mouse, i.t.) for up to 9 d. For BC-1215 treatment, a stock solution (5 mg/ml) was added to drinking water (containing 2% sucrose) to the final concentration of 30 μg/ml. Lung mechanics were measured at day 5 using a FlexiVent (**A–C**). **D**. Survival studies of mice administered i.t. with H1N1 (10^5 pfu/mouse, n=8 mice/group). Mice were then euthanized and lungs were lavaged with saline, harvested, and then homogenized. Cell counts and lavage protein were measured in (**E, F**). **G**. Gross images of lungs from vehicle or BC-1215 treated mice. **H**. H&E staining was performed on lung samples. The data represent n=5–8 mice/group, *P<0.05 versus H1N1.

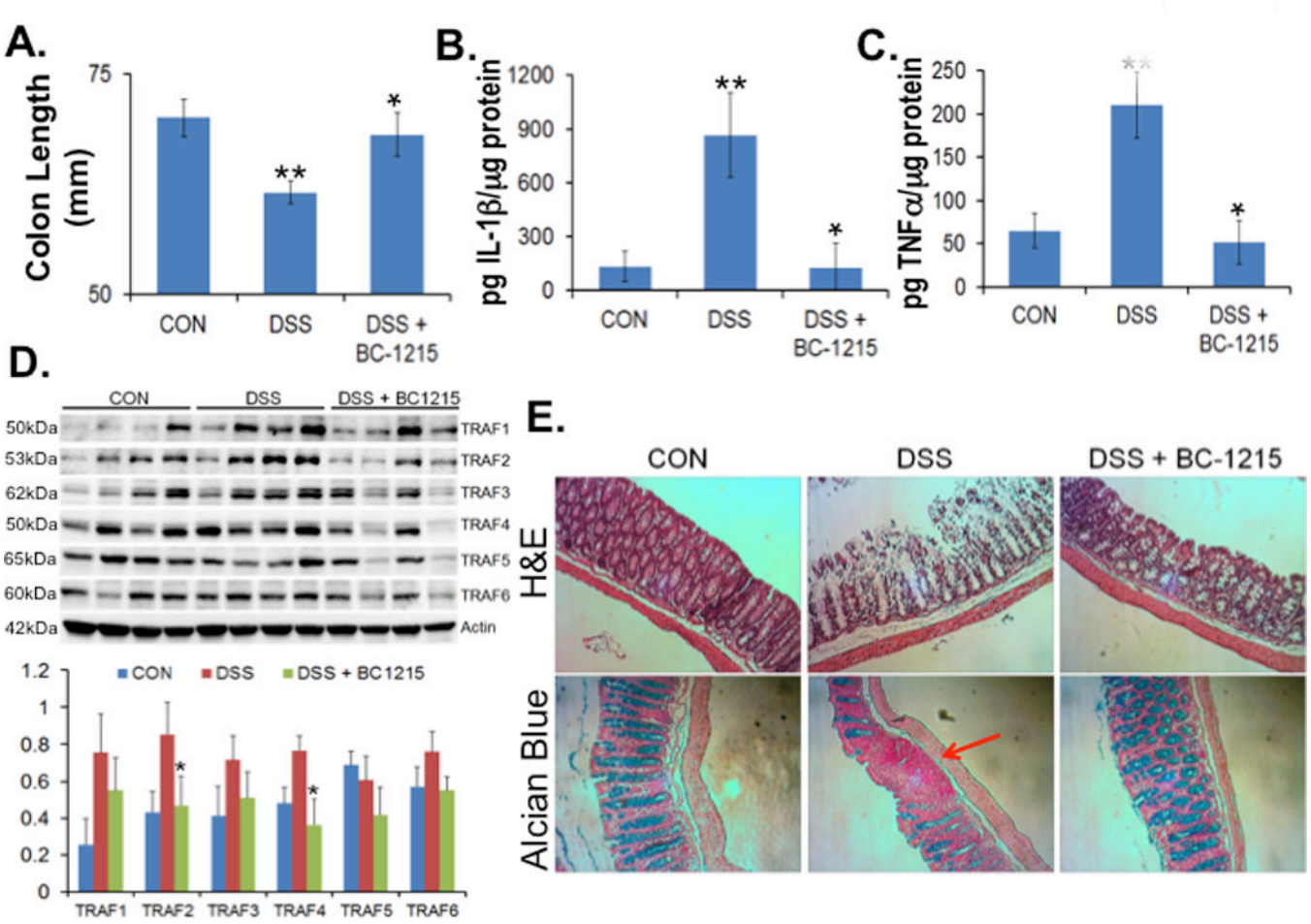

Figure 6. BC-1215 reduces DSS induced colonic inflammation

A–E. C57BL6 mice were fed with water *ad lib* containing 3.5% dextran sulfate sodium (DSS) for up to five days. Mice were treated with either vehicle (control [CON]) or BC-1215 (100 μg) daily (via an i.p. injection). Mice were then euthanized and the length of the colon was measured and graphed in (**A**). Colonic tissues were also analysed for IL1β (**B**), TNFα (**C**) and TRAF proteins by immunoblotting (**D**). **E.** H&E and Alcian blue staining were performed on colonic sections. The data represent n=4 mice/group, *P<0.05 versus DSS and **P<0.05 versus CON).

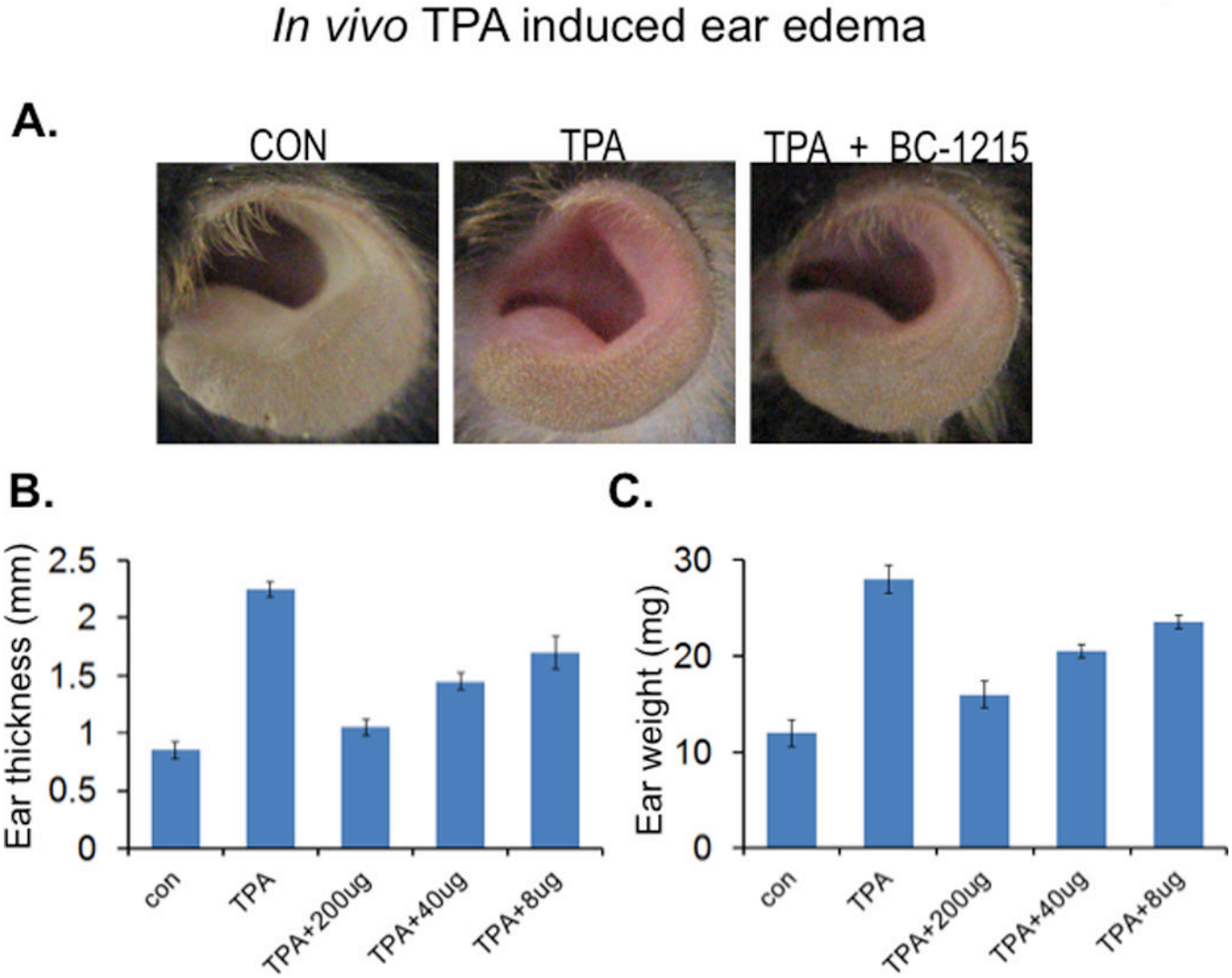

Figure 7. BC-1215 reduces TPA induced ear edema

A–C. C57BL6 mice were deeply anesthetized with ketamine (80–100 mg/kg i.p.) and xylazine (10 mg/kg i.p.). 20 μl of ethanol solution of BC-1215 was applied to ears at 8, 40, 200 ug/ear 30 min after TPA administration (2 μg/ear). Comparisons included equal volumes of ethanol (vehicle control, CON). 18 h after TPA administration, mice ears were imaged (**A**) before euthanization; the thickness of the ear was measured using a micrometer (**B**). Ear punch biopsies were also taken immediately, weighed and graphed (**C**).